Real-Time Implementation of a Discrete-Time Controller for a WMR*

R. Orosco-Guerrero†, M. Velasco-Villa, E. Aranda-Bricaire.
CINVESTAV-IPN
Departamento de Ingeniería Eléctrica
Sección de Mecatrónica
Apdo. 14-740, 07000, México DF, México
Tel: (+52) 55 57 47 38 44, Fax: (+52) 55 57 47 38 66
E-mail: {rorosco, velasco, earanda}@mail.cinvestav.mx.

Abstract

A discrete-time kinematic model and a control scheme for a two wheel differentially driven mobile robot are presented. The discrete-time control scheme proposed solves the path tracking problem based on two discrete-time linearizing control laws with different singular manifolds. The resulting control scheme is evaluated by real-time experiments over a low cost laboratory prototype.
Key words: Discrete-time modelling, mobile robot, discrete-time linearization, discrete-time control.

1 Introduction

Most of the controllers for nonlinear systems are designed by considering a continuous-time models. That produces continuous-time controllers, however, most of the controllers are digitally implemented and therefore they are actually operated in discrete time. The main reason to use continuous-time controllers over its discrete-time version is the complexity that involves the discretization of a nonlinear system. Wheeled Mobile Robots (WMR) belong to a class of nonlinear systems and their controllers are usually based on their continuous-time model. An exact discrete-time model for a particular case of WMR named "two-wheel differentially driven mobile robot" can be obtained by direct integration of its continuous-time model.

The control via feedback linearization is one of the control alternatives for nonlinear systems. There is a complete theory about this nonlinear control strategy [1, 2] that is developed by considering mainly the continuous-time nonlinear case. Several questions studied for continuous-time case can also be stated in the discrete-time context [3]. However, the solutions obtained for continuous-time systems are not always parallel to the solutions obtained for discrete-time systems since typical operations associated with continuous-time systems do not immediately apply for the discrete-time case. For the study of nonlinear discrete-time systems, see [1], Chapter 14 or [3] where the subject is treated more deeply. Also, different notions of feedback linearization are studied in [4].

There are several works where the continuous-time model of a two-wheel differentially driven mobile robot is used to design path-tracking control schemes as in [5, 6] where the results of a mobile robot controlled by a nonlinear linearizing feedback are presented. In the present work a discrete-time nonlinear control scheme for the same class of mobile robot is developed. This control scheme solves the path-tracking control problem by commutation between two discrete-time linearizing control laws.

The paper is organized as follows: In Section 2 the discrete-time model obtained from the continuous-time kinematic model of a two-wheel differentially driven mobile robot is presented. In Section 3 a path-tracking control via feedback linearization is presented. In Section 4 a real-time experiment with a laboratory prototype is carried out to show the performance of the proposed control. Finally the conclusions are presented in Section 5.

2 Discrete-time model

The wheeled mobile robot considered in this work is shown in Figure 1. This class of robots, called *two-wheel differentially driven mobile robot* consists of two parallel fixed wheels driven independently. A change of direction is obtained by the difference of velocity between the two wheels. The continuous-time kinematic model of this mobile robot is well

*Supported by CONACyT-México under Grant 42093.
†Supported by CONACyT-MEXICO.

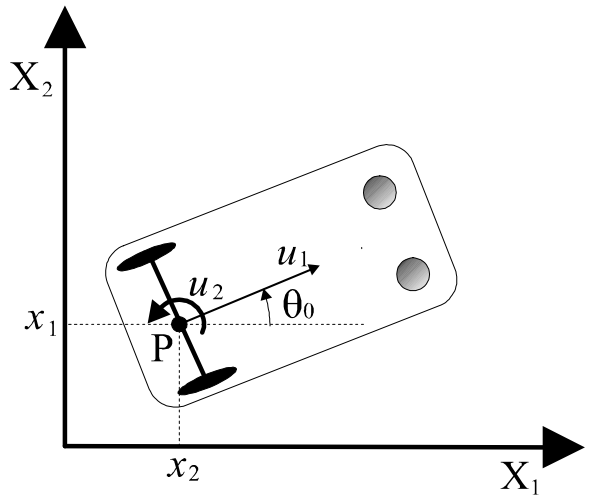

Figure 1: Two-wheel differentially driven mobile robot.

known in the literature [7], and it is given by

$$\begin{aligned} \dot{x}_1 &= u_1 \cos\theta_0 \\ \dot{x}_2 &= u_1 \sin\theta_0 \\ \dot{\theta}_0 &= u_2 \end{aligned} \tag{1}$$

where (x_1, x_2) represents the coordinates of the center of the axe of the actuated wheels on the plane (X_1, X_2) and θ_0 is the angle that the longitudinal axis of the robot makes with respect to the axis X_1. The input signal u_1 represents the linear velocity of the robot and u_2 its angular velocity.

A discrete model of the robot shown in Figure 1 can be obtained by direct integration of the continuous-time model (1). The resulting discrete-time model is given as,

$$\begin{aligned} x_1^+ &= x_1 + 2u_1\psi\cos\gamma \\ x_2^+ &= x_2 + 2u_1\psi\sin\gamma \\ \theta_0^+ &= \theta_0 + u_2 T. \end{aligned} \tag{2}$$

where

$$\begin{aligned} \psi &= \begin{cases} \frac{\sin\left(\frac{T}{2}u_2\right)}{\frac{u_2}{2}} & \text{if } u_2 \neq 0 \\ \frac{T}{2} & \text{if } u_2 = 0 \end{cases} \\ \gamma &= \theta_0 + \frac{T}{2}u_2. \end{aligned}$$

For the sake of simplicity the notation $\zeta^+ = \zeta(kT+T)$ and $\zeta = \zeta(kT)$ it is adopted.

Remark 2.1 *Note that,*

$$\lim_{u_2 \to 0} \frac{\sin\left(\frac{T}{2}u_2\right)}{u_2} = \frac{T}{2}$$

then the function ψ is continuous.

3 Discrete-time control scheme

In this section, a commutation control scheme for system (2) is proposed. The control strategy achieves the path-tracking of a desired trajectory of the two wheel differentially driven mobile robot based on the commutation between two discrete-time linearizing feedbacks. The main commutation feedback considers an output function that fully linearize system (2) while a complementary feedback that posses a different singular manifold is enabled when the main feedback is in the neighborhood of its respective singular manifold. The alternative feedback is designed by considering an output function that allow to linearize the input-output response of the system with a one dimensional stable internal dynamic.

In order to obtain the two linearizing control laws, it is proposed the dynamic extension,

$$\begin{aligned} \xi_1 &= \theta_0^-, \quad \xi_1^+ = \theta_0 \\ \xi_2 &= u_2, \quad \xi_2^+ = w_2 \\ w_1 &= u_1, \end{aligned} \tag{3}$$

where the notation $\zeta^- = \zeta(kT - T)$ is adopted. The dynamic extension (3) allow to rewrite (2) as the extended system,

$$x^+ = f(x, w) \tag{4}$$

where,

$$\begin{aligned} x &= [x_1, x_2, \xi_1, \theta_0, \xi_2]^T \\ w &= [w_1, w_2]^T \\ f(x,w) &= \begin{bmatrix} x_1 + 2\psi w_1 \cos\gamma \\ x_2 + 2\psi w_1 \sin\gamma \\ \theta_0 \\ \theta_0 + T\xi_2 \\ w_2 \end{bmatrix}. \end{aligned}$$

Remark 3.1 *In plain words, the dynamic extension (3) amounts to add one pure time delay in front of the input u_2, and to store the value at the previous time instant of the variable θ_0, in order to sinthetize the control law.*

The output function that fully linearize the system (4) is given by,

$$\bar{y} = \bar{h}(x) = \begin{bmatrix} x_1 \sin\gamma^- - x_2 \cos\gamma^- \\ \xi_1 \end{bmatrix} \tag{5}$$

where γ^- is given as,

$$\gamma^- = \frac{\theta_0 + \xi_1}{2}.$$

Considering the output function (5) a control feedback law that solves the path tracking problem

is obtained as,

$$\left[\begin{array}{c} w_1 \\ w_2 \end{array}\right] = \left[\begin{array}{c} \frac{1}{2\psi \sin\left(\frac{\theta_0-\bar{v}_2}{2}\right)}\left(x_1 \sin\bar{\phi} - x_2\cos\bar{\phi} - \bar{v}_1\right) \\ \frac{1}{T}\left(\bar{v}_2 - \theta_0 - T\xi_2\right) \end{array}\right] \tag{6}$$

where $\bar{\phi} = \frac{\bar{v}_2+\theta_0+T\xi_2}{2}$ and the new input variables $\bar{v}_1$ and $\bar{v}_2$ are proposed as,

$$\begin{aligned} \bar{v}_1 &= \bar{y}_{1d}^{[2]} + \bar{k}_1\bar{e}_1^{+} - \bar{k}_0\bar{e}_1 \\ \bar{v}_2 &= \bar{y}_{2d}^{[3]} - \bar{m}_2\bar{e}_2^{[2]} + \bar{m}_1\bar{e}_2^{+} - \bar{m}_0\bar{e}_2 \end{aligned}$$

with the output error $\bar{e} = \bar{y} - \bar{y}_d$. In order to simplify the notation, it will be considered the notation $\zeta^{[i]} = \zeta\left(kT + iT\right)$, $\zeta^{[-i]} = \zeta\left(kT - iT\right)$.

For the sake of conciseness the control law (6) designed for system (4), will be referred in the rest of the paper as $\bar{w}$.

Remark 3.2 *The sum of the scalar relative degrees of system (4)-(5) is equal to the dimension of (4), then feedback law (6) fully linearizes the system.*

Remark 3.3 *The control law $\bar{w}$ is not defined when the state belong to the singular manifold*

$$\bar{S} = \left\{(x,\xi) \in \mathbb{R}^5 \mid |\theta_0 - \bar{v}_2| = 2n\pi \text{ or } T\xi_2 = 2m\pi\right\} \tag{7}$$

for $n = 0, 1, 2, \ldots$ and $m = 1, 2, \ldots$.

The mentioned complementary feedback law is obtained by considering the output function

$$\tilde{h}\left(x\right) = \left[\begin{array}{c} \tilde{h}_1 \\ \tilde{h}_2 \end{array}\right] = \left[\begin{array}{c} x_1\cos\gamma^{-} + x_2\sin\gamma^{-} \\ \xi_1 \end{array}\right]. \tag{8}$$

This output function allows to obtain the feedback law,

$$\left[\begin{array}{c} w_1 \\ w_2 \end{array}\right] = \left[\begin{array}{c} \frac{1}{2\psi}(\tilde{v}_1 - x_1\cos\gamma - x_2\sin\gamma) \\ \frac{1}{T}(\tilde{v}_2 - \theta_0 - T\xi_2) \end{array}\right] \tag{9}$$

where the new inputs $\tilde{v}_1$ and $\tilde{v}_2$ are now proposed as,

$$\begin{aligned} \tilde{v}_1 &= \tilde{y}_{1d}^{+} + \tilde{k}_0\tilde{e}_1 \\ \bar{v}_2 &= \tilde{y}_{2d}^{[3]} - \tilde{m}_2\tilde{e}_2^{[2]} + \tilde{m}_1\tilde{e}_2^{+} - \tilde{m}_0\tilde{e}_2 \end{aligned}$$

with the output error $\tilde{e} = \tilde{y} - \tilde{y}_d$.

Again, for sake of conciseness the control law (9) design for system (4) will be referred in the rest of the paper as $\tilde{w}$.

Remark 3.4 *The sum of the scalar relative degrees of system (4)-(8) is equal to four, therefore the augmented system (4) posses a zero dynamic of dimension one.*

Remark 3.5 *The control law $\tilde{w}$ is not defined when the states belong to the singular manifold*

$$\tilde{S} = \left\{(x,\xi) \in \mathbb{R}^5 \mid T\xi_2 = 2m\pi \text{ for } m = 1, 2, \ldots\right\}. \tag{10}$$

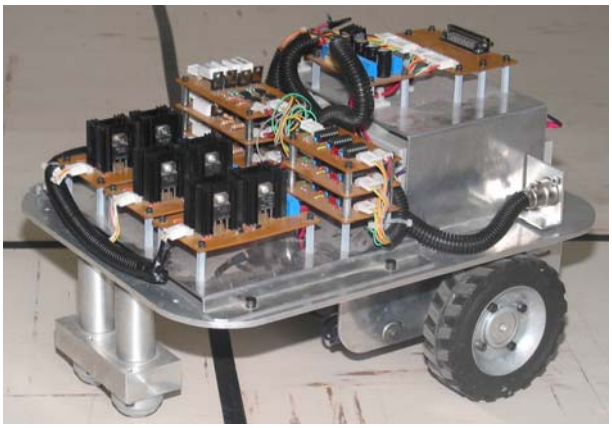

Figure 2: Laboratory prototype.

The control scheme proposed in this work is based on the commutation between control laws $\bar{w}$ and $\tilde{w}$. The singularities on the feedback (9) appear when the angular velocity of the robot ξ_2 is equal to a multiple of the sampling frequency (10), i.e., $\xi_2 = \frac{2m\pi}{T}$. For most sampling periods considered for practical discrete-time applications ($T \approx 0.1$s), these singularities can only appear for very high angular velocities of the mobile robot. Therefore, it can be reasonably assumed that this singularity does not appears in practical robots. From the above explanation it is proposed a commutation strategy that mainly takes into account the singularities produced by $\bar{S}$ instead of $\tilde{S}$. The commutation strategy takes the form,

$$w = \left\{\begin{array}{ll} \bar{w} & \text{if } \left|\sin\left(\theta_0 - \bar{v}_2\right)\right| \geq \varepsilon \\ \tilde{w} & \text{if } \left|\sin\left(\theta_0 - \bar{v}_2\right)\right| < \varepsilon \end{array}\right. \tag{11}$$

where ε is a small positive number that represent the threshold of commutation. The commutation scheme is designed considering that the control law $\bar{w}$ is enabled most of the time, and the control law $\tilde{w}$ is intended to act only when the state is on the neighborhood of the singularity $\sin\left(\theta_0 - \bar{v}_2\right) = 0$.

4 Real-time experiment results

In this Section the performance of the control commutation scheme presented in the preceding Section is evaluated by its implementation on a low cost laboratory prototype. The prototype is shown in Figure 2.

This Section is organized in two subsections, in the first one a general description of the laboratory prototype is given and in the second one the real-time results obtained are presented.

4.1 Prototype description

The experimental validation of the proposed control scheme has been performed using a laboratory prototype, a general description is presented in the following lines. The robot's wheels have a radius of $r = 6.5$cm and are mounted on an axle of length $l = 14.4$cm. Two passive omnidirectional wheels are placed on the front part of the vehicle. The aluminum chassis measures $42 \times 32 \times 26$cm (l/w/h) and supports two motors, transmission elements, power electronics, and a 12-V battery. Each motor has an incremental encoder counting $n_e = 1000$pulses/turn.

The prototype is controlled by a dSPACE Floating-Point Controller Board DS1102 that is based on the Texas Instrument TMS320C31 DSP. This board is placed on a 1-GHz Pentium III PC, with control algorithms written in Matlab's SIMULINK. The dSPACE Control Desk software provides a user interface with real-time visualization. The Controller Board communicates through multiwire cable with the electronics on the robot. The two wheels of the WMR are driven by a PWM signals sent by the DS1102 Board and their encoders measure the angular displacements $\Delta\phi_R$ and $\Delta\phi_L$ on the motors for odometric computation.

The velocity control of the two motors is done by means of a PID controllers implemented on the DS1102 Board. This controllers have a coulomb plus viscous friction compensation block. Filtering algoritms, potentiometer data adaptation and posture reconstruction from odometric data are implemented in the DS1102 Board.

The relationship between the control signals and the angular velocities of each motor are given by,

$$\begin{bmatrix} \omega_r \\ \omega_l \\ \omega_s \end{bmatrix} = \begin{bmatrix} \frac{r}{2} & \frac{r}{2} & 0 \\ \frac{r}{2l} & \frac{r}{2l} & 0 \\ 0 & 0 & 1 \end{bmatrix} \begin{bmatrix} u_1 \\ u_2 \\ u_3 \end{bmatrix}$$

where ω_r and ω_l represent the angular velocity of right and left wheels of the tractor and ω_s is the angular velocity of the motor on the axle of the trailer wheel.

4.2 Real-time experiment results

This Subsection is devoted to present the results obtained by the real-time implementation of the discrete-time control scheme (11) applied to the low cost laboratory prototype described in the previous Subsection.

The experiments were carried out by considering the following coefficients for $\bar{v}$ and $\tilde{v}$,

$$\begin{array}{ll} \bar{m}_0 = \tilde{m}_0 = 0.0893 & \bar{k}_0 = \tilde{k}_0 = 0.989 \\ \bar{m}_1 = \tilde{m}_1 = 1.082 & \bar{k}_1 = 1.989, \\ \bar{m}_2 = \tilde{m}_2 = 1.99. & \end{array}$$

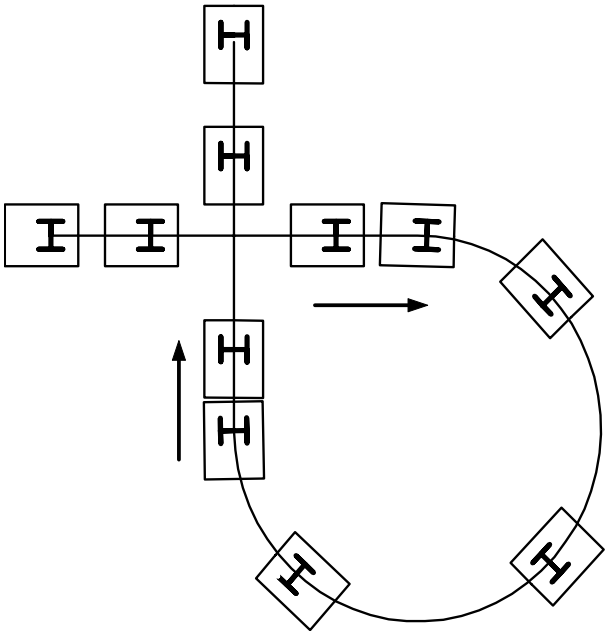

Figure 3: Two wheels differentialy driven mobile robot following a prescribed trajectory.

It was used the commutation threshold $\varepsilon = 0.05$ and the initial values for the state errors $e_1 = x_1 - x_{1d}$, $e_2 = x_2 - x_{2d}$, $e_3 = \theta_0 - \theta_{0d}$ were set to zero.

The prescribed trajectory is composed by two straight lines and a circumference arc (see Figure 3). This trajectory contains singular points for which the control law $\bar{w}$ is not well defined, this allow to evaluate the performance of the control scheme (11) by commutations between $\bar{w}$ and $\tilde{w}$. The mobile robot completes the desired trajectory in seventy seconds, the first twenty with the horizontal line, the next thirty with the circumference arc and the last twenty with the vertical line.

The position on the workspace of the mobile robot at different sampling instants (each 7s) is shown in Figure 3. The initial position of the robot at the beginning of the desired trajectory is accordingly with the considered initial errors.

The commutation between the feedback laws $\bar{w}$ and $\tilde{w}$ is shown in Figure 4 where the alternation of the two control laws during the experiment is presented.

The evolution of the input signals w_1 and w_2 is shown in Figure 5 where it is possible to see that the commutation between the feedback laws $\bar{w}$ and $\tilde{w}$ does not influence the control signals w_1 and w_2. Some peaks can be observe at the points of the trajectory where the straight lines and the circumference arc are joined. These peaks are produced by the coulomb friction of the motors because the robot velocity is zero at this points.

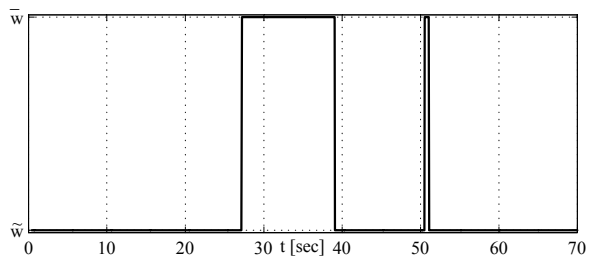

Figure 4: Commutation between controls.

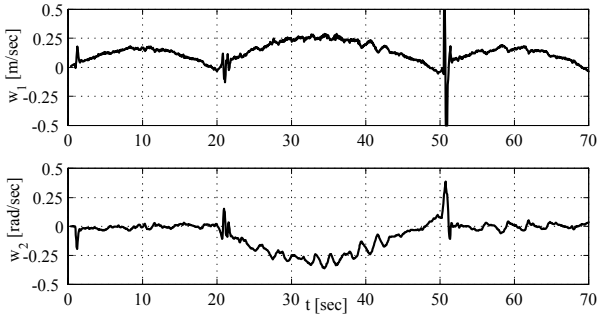

Figure 5: Evolution of input signals w_1 and w_2.

The voltage applied to each motor of the wheels is shown in Figure 6. Some peaks can be observe at the same times that the peaks on the controllers as is expected. Each of this voltage signals are provided by the PID controller that control the velocity of the wheel motors.

The evolution of the state errors e_1, e_2, e_3 is shown in Figure 7. The state errors e_1 and e_2 have three different behaviors corresponding to each part of the trajectory. The error state e_3 (Corresponding to the output error $\bar{e}_2 = \tilde{e}_2$) is around zero as is

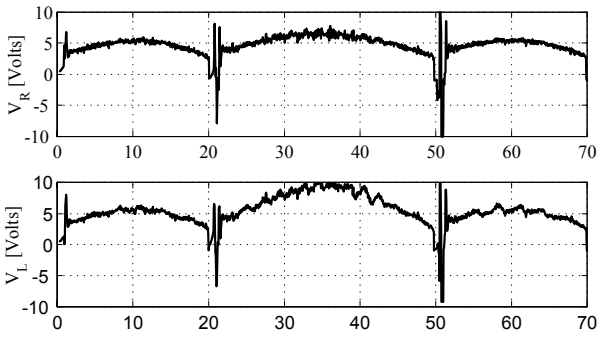

Figure 6: Evolution of the voltage applied to the Rigth Wheel Motor (V_R) and the Left Wheel Motor (V_R).

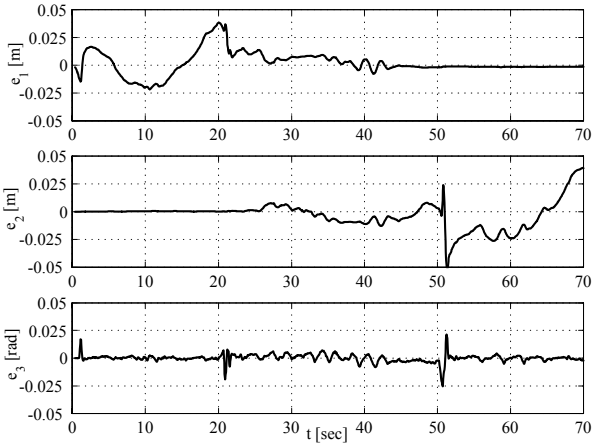

Figure 7: Evolution of the state errors e_1, e_2, e_3.

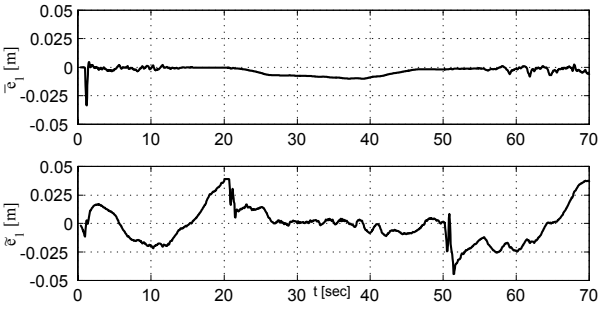

Figure 8: Evolution of the output errors $\bar{e}_1$ and $\tilde{e}_1$.

expected with a small peaks at the trajectory joints.

The evolution of the output errors $\bar{e}_1$ and $\tilde{e}_1$ is shown in Figure 8. This errors remain around zero as is expected.

5 Conclusions

In this paper a path-tracking control scheme based on the exact discrete-time model of a two wheel differentially driven mobile robot is presented. the proposed control scheme is based on the commutation of two nonlinear feedback laws that are designed for the discrete-time model of the WMR based on a linearization strategy of the (input-output) response of the system.

The real-time experiments were carried out over a low cost laboratory prototype. The obtained results show a good performance of the proposed control strategy and that the commutation between the considered feedbacks does not affect the evolution of the signals.

References

[1] H. Nijmeijer and A. Van Der Schaft. *Nonlinear Dynamical Control Systems*. Springer-Verlag, New York, 1990.

[2] A. Isidori. *Nonlinear Control Systems*. Springer-Verlag, London, third edition, 1995.

[3] Ülle Kotta. *Inversion Method in the Discrete-Time Nonlinear Control Systems Synthesis Problems*. Lecture Notes in Control and Information Sciences 205. Springer-Verlag, London, 1995.

[4] E. Aranda-Bricaire, U. Kotta, and C. H. Moog. Linearization of discrete-time systems. *SIAM Journal on Control and Optimization*, Vol. 34(No. 6):1999–2023, 1996.

[5] E. Aranda-Bricaire, T. Salgado-Jiménez, and M. Velasco-Villa. Control no lineal discontinuo de un robot móvil. *Computación y sistemas*, (Número especial):42–49, Dic 2002.

[6] G. Oriolo, A. De Luca, and M. Venditteli. WMR control via dynamic feedback linearization: Design, implementation, and experimental validation. *IEEE Transaction on Control Systems Technology*, Vol. 10(No. 6):835–852, 2002.

[7] C. Canudas de Wit, B. Siciliano, G. Bastin, B. Brogliato, G. Campion, B. D'Andrea-Novel, A. De Luca, W. Khalil, R. Lozano, R. Ortega, C. Samson, and P. Tomei. *Theory of Robot Control*. Springer-Verlag, London, 1996.